9. Stratospheric Aerosol Measurements

Experiment MA-007

T. J. Pepin,[a†] M. P. McCormick,[b] W. P. Chu,[c] F. Simon,[a] T. J. Swissler,[d] R. R. Adams,[b] K. H. Crumbly,[b] and W. H. Fuller, Jr.[b]

ABSTRACT

The Apollo-Soyuz Test Project Stratospheric Aerosol Measurements Experiment was flown to demonstrate that direct solar occultation measurements by photometers and from photographs can be used for defining stratospheric aerosol concentrations. Supporting ground-truth data provided by laser radar and balloonborne dustsonde are used with the remote-sensing data to investigate the uniqueness of aerosol optical models. The results show a 1.5 times higher peak aerosol concentration in the Northern Hemisphere than in the Southern Hemisphere.

INTRODUCTION

This experiment was designed to demonstrate the feasibility of remotely sensing aerosols in the stratosphere from a low-orbiting manned spacecraft. Increasing interest in the stratosphere has led to the investigation of methods for remote sensing from Earth-orbiting satellites. Information gained from the Stratospheric Aerosol Measurements (SAM) Experiment performed during the Apollo-Soyuz Test Project (ASTP) mission will be used in the design of remote-sensing equipment for future satellite missions.

The instrument used for making these stratospheric aerosol measurements consisted of a photometer and associated electronics that provided a signal to the command module (CM) telemetry system. A Hasselblad data camera (HDC) equipped with special infrared (IR) film and filter was used to photograph the sunset and sunrise events. The experiment technique involved directly measuring solar intensity (photometer) and Sun shape (photographs) in the spectral region centered at approximately 0.84 μm. Immediately before satellite night, as the spacecraft approached the shadow of the Earth, the line of sight to the Sun passed first through the upper layers of the atmosphere and then steadily down into the lower layers of the troposphere. During the 1.5 minutes (approximately) required for the instrument line of sight to pass through the lower 150 km of the atmosphere, the solar intensity was recorded by the photometer, and solar disk shape changes were recorded in photographs. The same set of measurements was made at satellite dawn as the spacecraft emerged from the shadow of the Earth.

The total extinction coefficient was obtained from the variation of the solar intensity as a function of total airmass distributed along the line of sight. At the effective wavelength of the photometer and the photographic system, the extinction

[a]University of Wyoming.

[b]NASA Langley Research Center.

[c]Old Dominion University.

[d]Systems and Applied Sciences Corporation.

[†]Principal Investigator.

was principally produced by the atmospheric aerosols; the measurements are being used to determine the aerosol concentration.

To verify the performance of the SAM Experiment, ground-truth data were acquired by dustsonde (a balloonborne aerosol optical counter) and a lidar system (ground-based laser radar). The dustsonde was flown from the Richards-Gebaur Air Force Base (lat. 38.8° N, long. 94.7° W) near Kansas City, Missouri, at the same time and place of the ASTP second sunset SAM. The lidar measurements were also made from Richards-Gebaur Air Force Base on Earth nights bracketing and during the second sunset SAM.

THE SAM INSTRUMENT

The photometer (fig. 9-1) used for the SAM Experiment utilizes a pin diode detector having a 10° field of view (FOV), which was used to look at the Sun through the CM window at a wavelength centered at approximately 0.84 μm. The detector was used in the photovoltaic mode to detect the solar signal, and samples were taken at a rate of 10 samples/sec using a 12-bit analog-to-digital converter. The signal output of the converter was recorded and transmitted by the CM data system.

The photometer was equipped with a projection sight system consisting of a post whose shadow was projected onto a grid that could be observed by the astronaut to ensure that the photometer system was properly alined with respect to the Sun. The instrument also included a green light to verify that the power was properly connected and included a switch that the astronaut could activate to send a known signal over the telemetry system to verify proper installation of the photometer in the CM.

CAMERA SYSTEM

The photographic portion of the experiment consisted of a series of timed IR photographs of spacecraft sunrises and sunsets taken through the CM window with an HDC. The 250-mm-focal-length (12.5° by 12.5° FOV), f/5.6 lens was fitted with a quality glass IR filter capable of obtaining at least three orders of magnitude blocking in the visible and the ultraviolet. Kodak multispectral IR aerial film (ESTAR-AH base) SO-289 was used in two 70-mm Hasselblad magazines. Each magazine contained film for 50 frames with an additional 1 m reserved for sensitometric calibration exposures. The HDC had a self-contained battery power supply for shutter activation and film advance. An onboard intervalometer provided a contact closure to the HDC every 2.5 seconds during the experiment to trigger the camera automatically. Timing with SAM data was to be provided by an audio channel of the spacecraft tape recorder.

BALLOONBORNE "DUSTSONDE"

Figure 9-2 is a schematic drawing of the University of Wyoming balloonborne dustsonde used in this program for the ground-truth *in situ* aerosol measurement that was made from the Richards-Gebaur Air Force Base. The mode of operation of the dustsonde is described in the following discussion.

Air sampled on balloon ascent and parachute descent is pumped at approximately 0.75 liter/min in a well-defined stream through the focal point of the condenser lens in the 2.5-liter scattering chamber where individual particles scatter light into the microscopes. The light pulses that can be observed with the microscopes are detected and amplified by the photomultipliers. By pulse-height discrimination and careful laboratory calibration with aerosols of known size and index of refraction, the integral concentration of aerosol particles larger than 0.3 and 0.5 μm in diameter can be determined.

Two photomultipliers were used to enhance the signal-to-noise ratio by requiring coincident events from the two detectors. The background noise for the system was mainly due to Rayleigh scattering from the air molecules in the chamber at low altitude and from cosmic-ray scintillation in the photomultiplier glass at high altitudes. The background was measured approximately every 15 minutes during the flight by passing filtered air through the chamber. For the system used in the Kansas City flight, the background was negligible

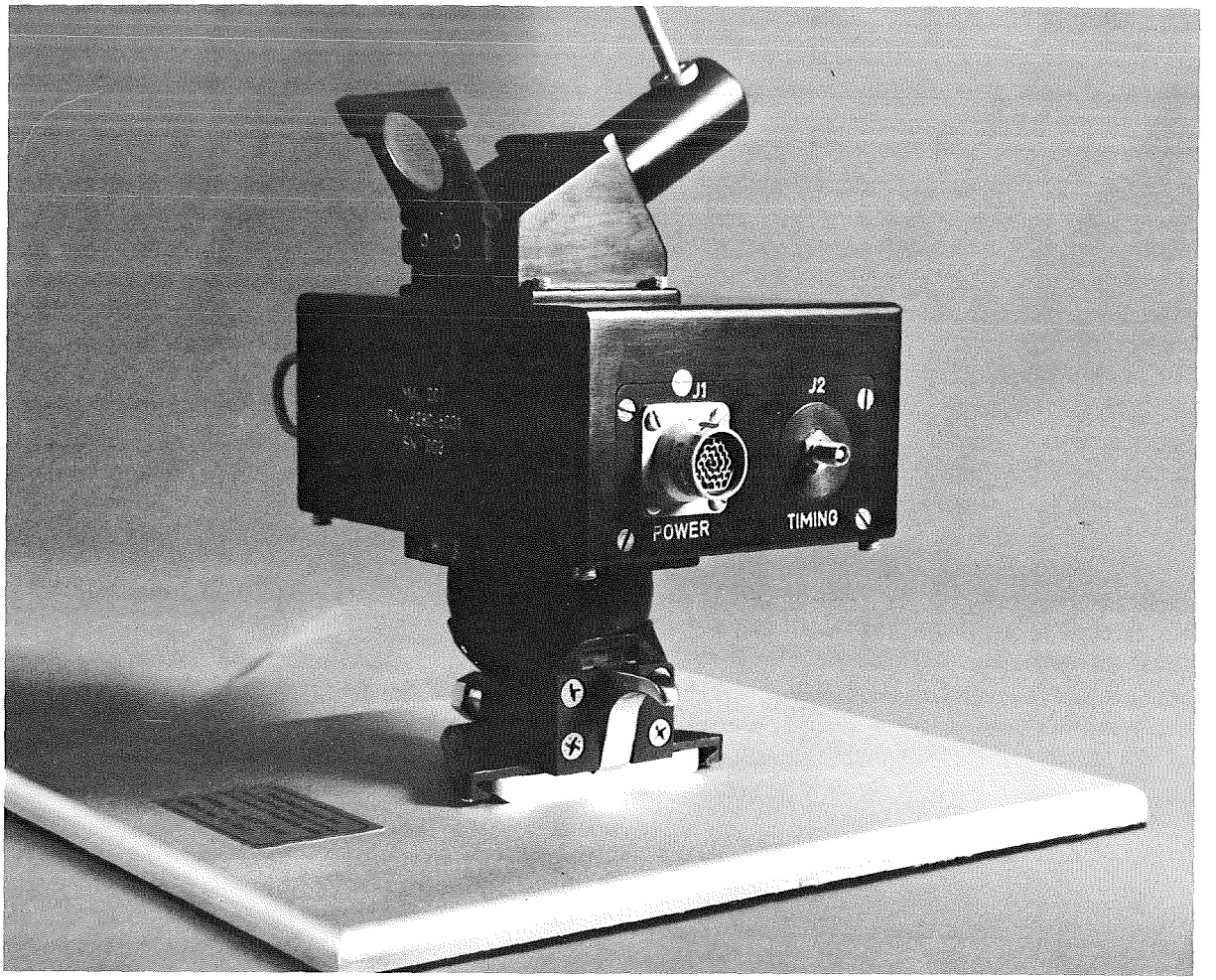

FIGURE 9-1.—The photometer used for making stratospheric aerosol measurements.

above a 10-km altitude. Corrections for the background have been used below this altitude. The dustsonde was also equipped with a rawinsonde temperature element for recording the atmospheric temperature profile (ref. 9-1).

LIDAR

Ground-based lidar measurements were used as part of the ground truth for the experiment. Generally, laser radars operate in the following manner. A Q-switched laser emits a pulse of nearly monochromatic light approximately 30

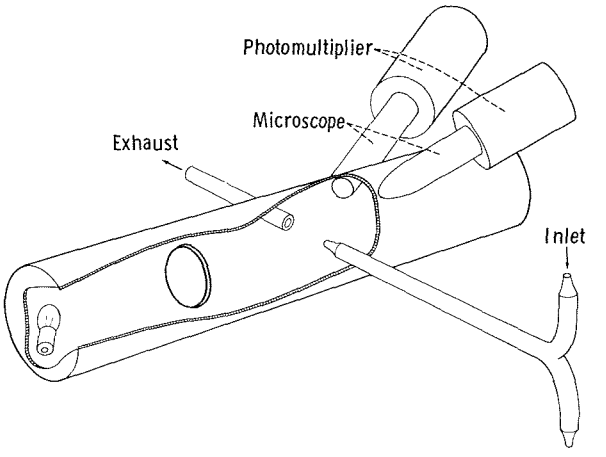

FIGURE 9-2.—Schematic drawing of the University of Wyoming dustsonde used for ground-truth measurements.

nanoseconds in duration. Molecules and suspended particulate matter (aerosols) scatter and/or absorb this radiation as the pulse propagates through the atmosphere. A small portion of this light is scattered directly back toward the laser. A receiver composed of mirrors and/or lenses collects this backscattered radiation and diverts it onto a photodetector, the output of which is measured as a function of elapsed time after laser emission, or range. The backscattered energy incident on the photodetector is examined spectrally at or near the laser output wavelength with color filters, interference filters, or spectrometers. This enhances the signal-to-noise ratio by reducing unwanted background radiation and determines whether elastic or inelastic techniques will be used.

The lidar measurements for the SAM experiment were provided by the NASA Langley Research Center (LaRC) 122-cm (48 in.) laser radar system (fig. 9-3), which consists of two temperature-controlled lasers (ruby and neodymium-doped glass) mounted on either side of an f/10 Cassegrainian-configured telescope composed of a 122-cm (48 in.) diameter, f/2, all-metal primary and a 25.4-cm (10 in.) diameter secondary. The output from the detector package is recorded by a high-speed data acquisition system. Analog signals are amplified and bandwidth limited, digitized at a 5- or 10-MHz rate with 8-bit accuracy, and recorded on magnetic tape. A 16-bit-word storage computer is used to control the data acquisition system and to process the data. An X-band microwave radar, coincident with the laser system axis, is used to ensure safe operation in the atmosphere. A rotating shutter reduces laser fluorescence after Q switching. The entire system is mobile and can scan in elevation and azimuth at a slew rate of 1°/sec (ref. 9-2).

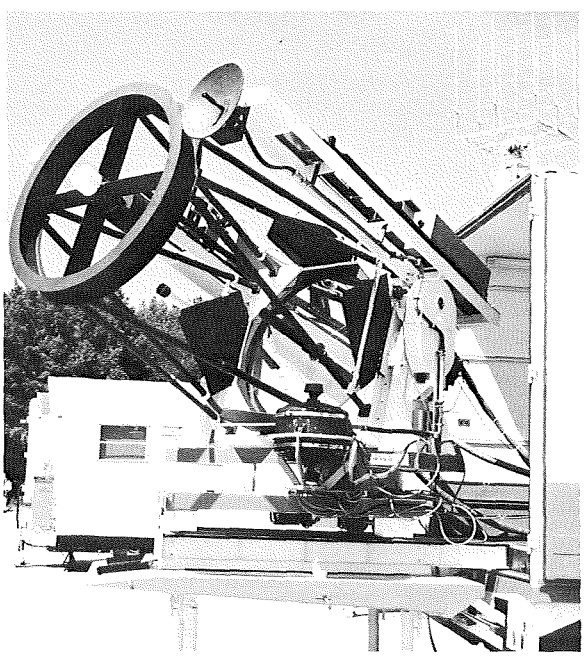

FIGURE 9-3.—The NASA Langley Research Center 122-cm (48 in.) lidar system.

METHOD OF INVERSION

The SAM inversion scheme employed for the inversion of the SAM results presented in this paper is based on an onionskin model of the atmosphere. For this model, the atmosphere is divided into a number of homogeneous, spherical layers that are considered to have uniform aerosol concentrations. Figure 9-4(a) shows a cross section of the measurement geometry and illustrates the path lengths of solar rays at different atmospheric layers. Fig. 9-4(b) shows the inversion geometry and illustrates the solar intensity contribution transmitted through the different layers as seen from the ASTP instrument during a sunset event.

As the bottom limb of the Sun becomes tangent to each of the layers of the onionskin atmospheric model, the intensity can be computed from limb darkening and refraction by summing the intensities over the layers above. For example, following the notation for the layers identified in figures 9-4(a) and 9-4(b), one finds that when the lower limb is tangent to the first and second layers, the observed intensities are given by

$$\left.\begin{aligned} I_1 &= I_{10}^{\odot} + I_{11} \\ I_2 &= I_{20}^{\odot} + I_{21} + I_{22} \end{aligned}\right\} \qquad (9\text{-}1)$$

where, in general, I_1 and I_2 are the observed intensities and $I_{10}^{\odot}$ and $I_{20}^{\odot}$ are the intensities above the upper layer of the inversion model (above the point at which extinction is observed). The intensities I_{11}, I_{21}, and I_{22} are the transmitted intensities to be determined by inversion. Using the Lambert-Beer law, equation (9-1) can be written in the form

$$\left.\begin{aligned} I_1 &= I_{10}^{\odot} + I_{11}^{\odot} \exp\left(-\beta_1 P_{11}\right) \\ I_2 &= I_{20}^{\odot} + I_{21}^{\odot} \exp\left(-\beta_1 P_{11}\right) + I_{22}^{\odot} \exp\left(-\beta_1 P_{21} - \beta_2 P_{22}\right) \end{aligned}\right\} \quad (9\text{-}2)$$

where $I_{ni}^{\odot}$ is the portion of the unattenuated solar intensity through the i-th layer that contributes to the observed intensity I_n; P_{ij} is the path length in the j-th layer for the solar ray tangent to the i-th layer; and β_i is the total extinction at the wavelength of the SAM system in the i-th layer. Equation (9-2) yields

$$\left.\begin{aligned} \beta_1 &= \frac{-1}{P_{11}} \ln\left(\frac{I_1 - I_{10}^{\odot}}{I_{11}^{\odot}}\right) \\ \beta_2 &= \frac{-1}{P_{22}} \ln\left(\frac{I_2 - I_{20}^{\odot} - I_{21}^{\odot} \exp\left(-\beta_1 P_{11}\right)}{I_{22}^{\odot}}\right) - \beta_1 \frac{P_{21}}{P_{22}} \end{aligned}\right\} \quad (9\text{-}3)$$

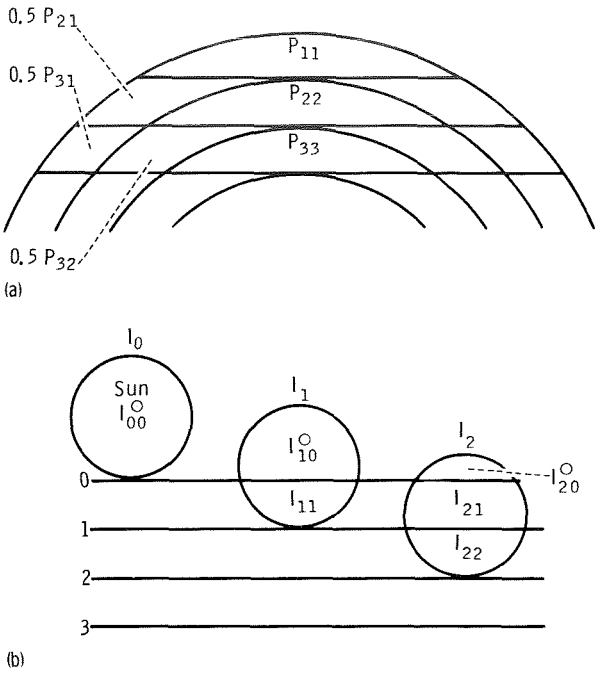

FIGURE 9-4.—Diagram of atmospheric model and inversion geometry. (a) Cross section of the onionskin atmospheric model showing the ray path lengths, where P_{ij} is the path length in the j-th layer for the solar ray tangent to the i-th layer. (b) Inversion geometry showing the contributions to the total transmitted Sun intensity, where I_n is the observed intensity for the n-th layer, I_{11}, I_{21}, and I_{22} are the transmitted intensities to be determined by inversion, and $I_{ni}^{\odot}$ is the portion of the unattenuated solar intensity that contributes to I_n.

This process can be continued as the sunset event occurs, thus allowing the determination of the vertical profile of the total extinction. The aerosol extinction profile can then be obtained by subtracting the molecular extinction contribution.

RESULTS

Photometry

The SAM Experiment was designed to observe four events on July 22, 1975. During Apollo revolution 95, measurements were made of a sunset observation (00:07:04 UT) off the coast of New Jersey (lat. 39°10′ N, long. 72°45′ W)[1] and of a sunrise observation (00:45:52 UT) over the Indian Ocean off the coast of Australia (lat. 43′ S, long. 99°55′ E). During Apollo revolution 96, a sunset observation (01:37:52 UT) was taken near Kansas City, Missouri (lat. 38°57′ N, long. 95°06′ W), followed by a sunrise observation (02:14:39 UT) over the Indian Ocean (lat. 42°55′ S, long. 77°39′ E). The SAM photometer was used to obtain radiometric measurements during each of these four events, and the measured photometric intensities have been inverted using the inversion procedure outlined previously to obtain total extinction as a function of altitude. Figures 9-5(a) and 9-5(b) illustrate the inverted results for the sunset events and sunrise events, respectively. The sunrise events took place in the Southern Hemisphere; the sunset events, in the Northern Hemisphere. The total extinction is greater at the

[1]These are the geometric coordinates of the tangent point of the 0-km-altitude grazing ray of the Sun.

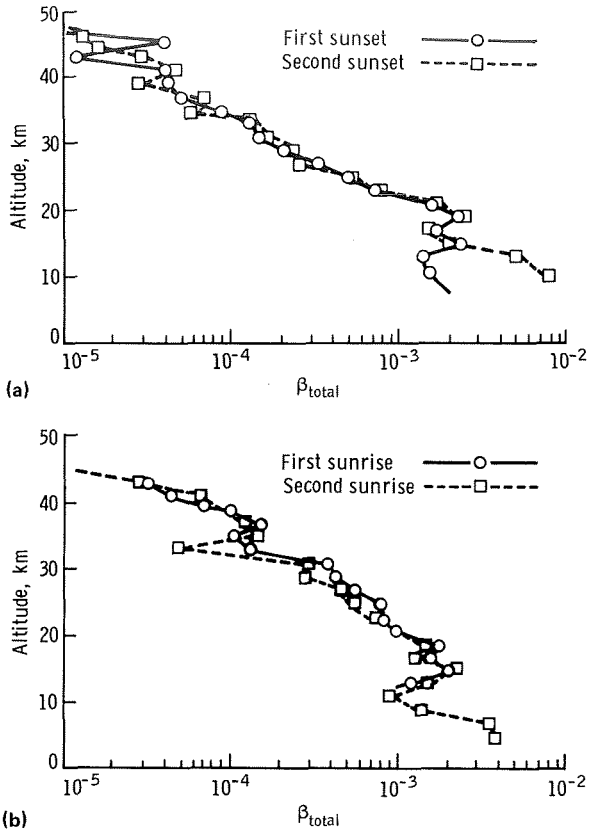

FIGURE 9-5.—Inverted total extinction (β_{total}) profiles for the four events observed. (a) First and second sunset events, Northern Hemisphere. (b) First and second sunrise events, Southern Hemisphere.

peak of the stratospheric aerosol layer in the Northern Hemisphere than was observed for the Southern Hemisphere by a factor of 1.5. This difference is interpreted as being due to the difference in aerosol content at the time of the ASTP flight. The difference in aerosol content is believed to be due to the injection of material from the Volcan de Fuego in Guatemala (lat. 14.5° N, long. 90.9° W), which erupted in October 1974 (ref. 9-3). The general meridional circulation of injected mass into the atmosphere would normally be northward during the fall and winter seasons in the Northern Hemisphere. This movement reverses in the summer, accounting for the buildup of aerosols in the Southern Hemisphere. This cross-hemispheric transport was beginning at the time of the ASTP mission. Dustsonde observations by Laby[2] near Melbourne, Australia, were made in April and August of 1975. The April flight showed low aerosol concentration, whereas the August flight showed a factor of 3.5 enhancement in the peak of the stratospheric aerosol concentration. These results are consistent with the three-dimensional circulation model of Cunnold et al. (ref. 9-4).

Photography

Photographs were made of the first sunrise and the second sunset with the HDC. Figure 9-6 is a composite of frames AST-28-2400 to AST-28-2406 taken during the first sunrise. These photographs have been printed with high contrast to show the observed refracted images of the solar disk and have been superimposed on a grid showing the horizon and tangent altitudes. Figure 9-7 shows frame AST-28-2402, an "isodensity tracing" of this frame, and an outline of the theoretical computed shape of the Sun as expected for the orbital and atmospheric conditions present. The distribution of the observed isophotes is due to limb darkening, extinction by atmospheric constituents, and the effects of refraction. These photographs confirm, at spacecraft altitude, that effects due to refraction must be considered in the design of solar occultation experiments. The photographs taken during the SAM events are currently being analyzed to substantiate theoretical models that are under development for use in future occultation experiments.

Ground-Truth Data

Data from the dustsonde balloon flight launched on July 21, 1975, at 23:58 UT are shown in figures 9-8 to 9-10. Figure 9-8 contains the measured temperature profile, figure 9-9 illustrates the measured aerosol concentration as a function of altitude for particles larger than 0.3 μm in diameter, and figure 9-10 shows the aerosol

[2]Private communication, 1975.

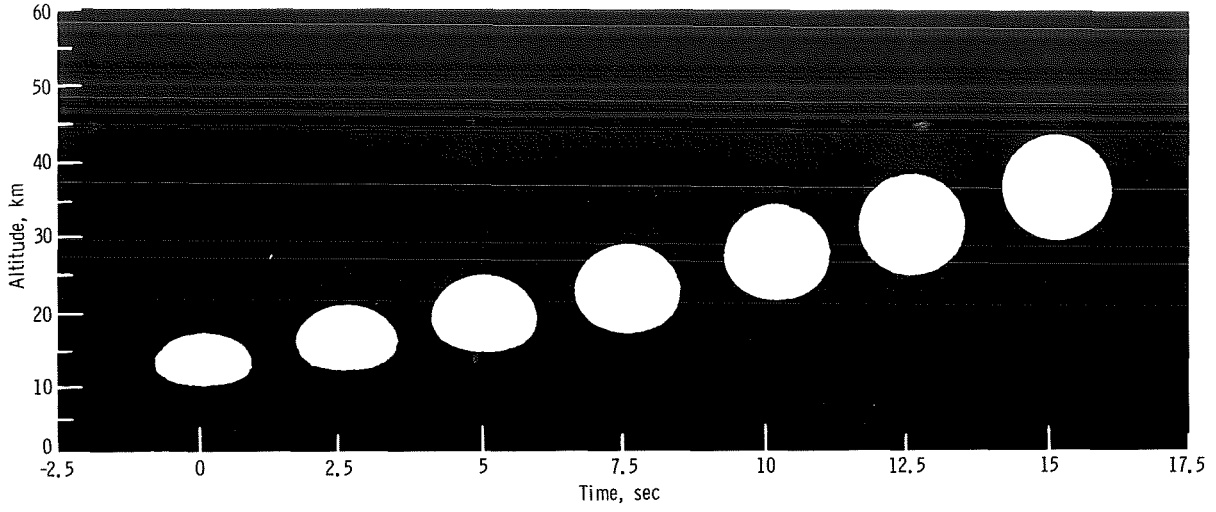

FIGURE 9-6.—Composite of photographs taken during first sunrise event (AST-28-2400 to 2406).

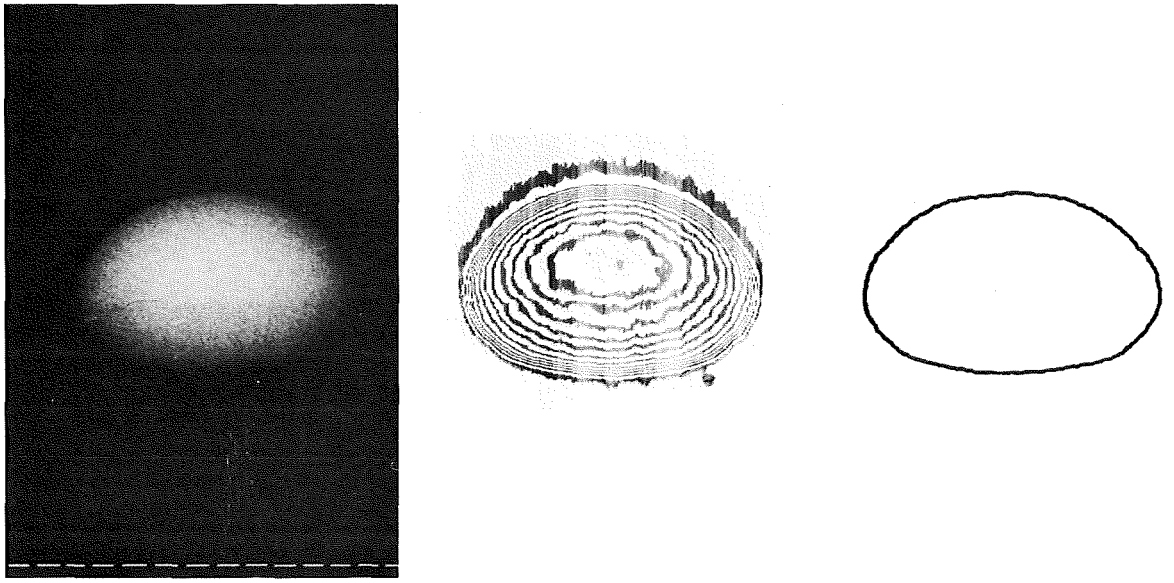

FIGURE 9-7.—Sun-shape comparisons. (a) High-contrast Sun photograph (AST-28-2402). (b) Isodensity tracing. (c) Expected refracted Sun shape.

count ratio (ratio of particles greater than 0.3 μm in diameter to particles greater than 0.5 μm in diameter) as a function of altitude.

The LaRC lidar system was used during the nights of July 22 and July 23 to obtain laser backscatter measurements of the stratospheric aerosols. Figure 9-11 shows the backscatter ratios obtained during the measurements made on July 23 at 07:30 UT, and figure 9-12 shows the measured backscatter ratios obtained on July 22 at 04:51 UT. (Backscatter ratio is the ratio of total observed backscatter to molecular backscatter.)

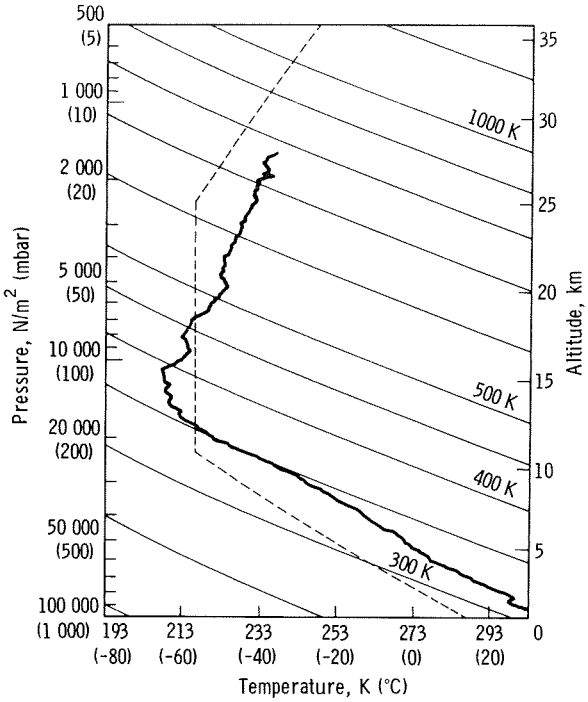

FIGURE 9-8.—Measured temperature profile above Kansas City, Missouri.

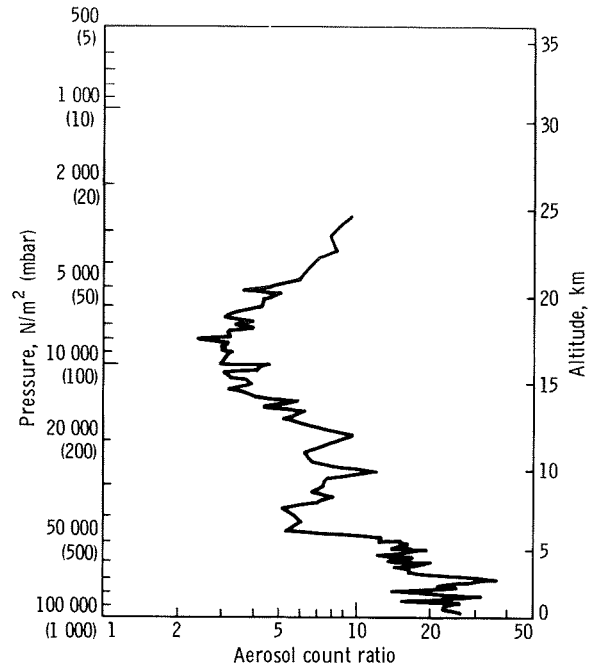

FIGURE 9-10.—Ratio of measured aerosol count for particles >0.3 μm diameter to particles >0.5 μm diameter above Kansas City, Missouri.

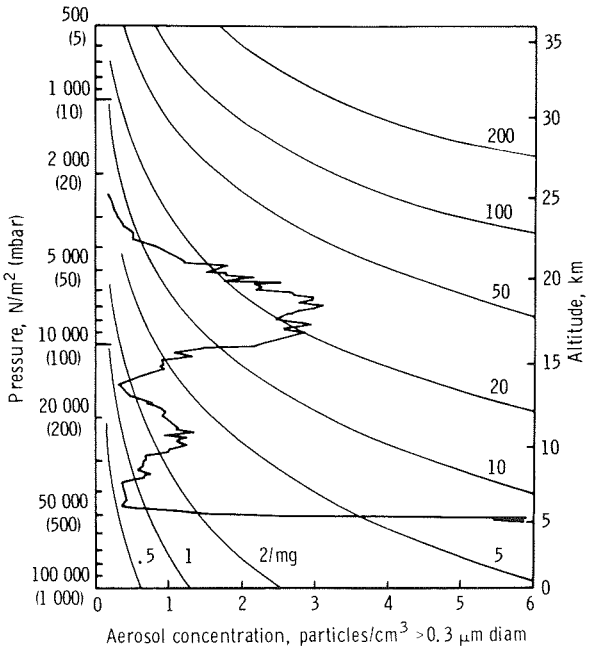

FIGURE 9-9.—Measured dustsonde aerosol concentration (>0.3 μm diameter) above Kansas City, Missouri. Curved lines indicate mixing ratio.

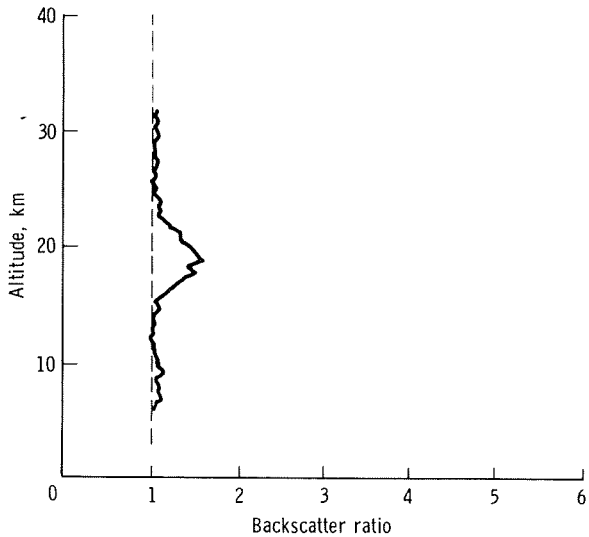

FIGURE 9-11.—Profile of lidar aerosol backscatter ratio taken at Kansas City, Missouri, on July 23, 1975, at 07:30 UT (normalized at 28.53 km).

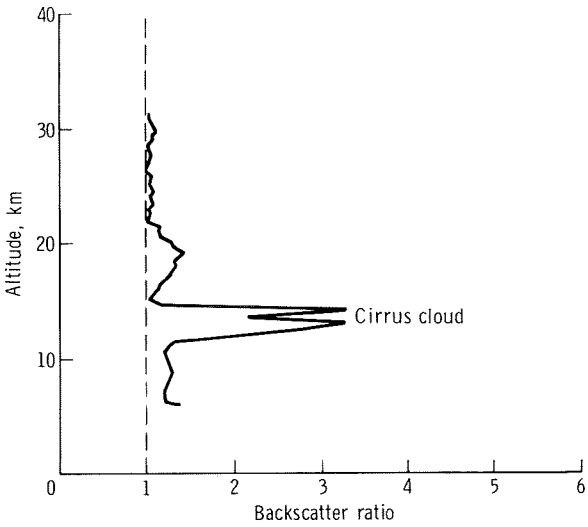

FIGURE 9-12.—Profile of lidar aerosol backscatter ratio taken at Kansas City, Missouri, on July 22, 1975, at 04:51 UT.

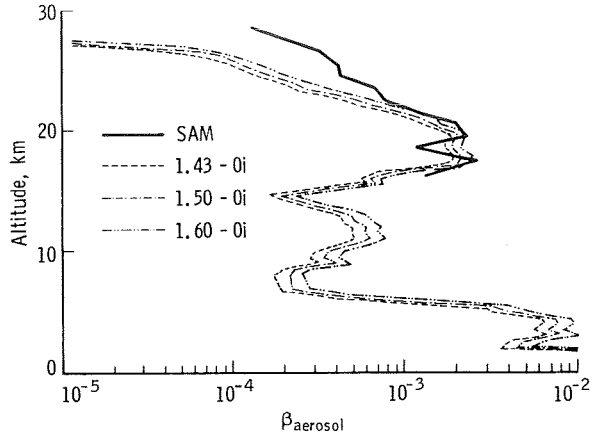

FIGURE 9-13.—Comparison of SAM results on July 22, 1975 (second sunset event), and Mie computations of dustsonde results on July 22, 1975, for different optical properties of the aerosols ($\beta_{aerosol}$ = aerosol extinction).

COMPARISON OF RESULTS

The balloon dustsonde measurements of number density of particles greater than 0.3 μm diameter and the aerosol count ratio have been used as a function of altitude to fit various size distributions. These size distributions have been used to predict the SAM photometer measurements of the aerosol extinction observed during the second sunset event and the lidar observations of the backscatter ratio. Figure 9-13 is a comparison plot of the SAM results and the Mie-scattering computations performed using the log-normal aerosol size distribution developed by Pinnick et al. (ref. 9-5). This distribution was adjusted as a function of altitude so that the total number and mode radius fit the dustsonde observations. For these calculations, the index of refraction for the stratospheric aerosol was taken to be $1.43 - 0i$, $1.50 - 0i$, and $1.60 - 0i$ (where $i = \sqrt{-1}$). The complex part of the index of refraction was found to have little effect on the extinction calculations.

Figures 9-14 and 9-15 show the comparisons between the lidar backscatter ratios observed on the nights of July 22 and July 23, respectively, and the computed backscatter ratios for index of refraction $1.43 - 0i$, $1.50 - 0i$, and $1.60 - 0i$. These backscatter ratios were computed using the same

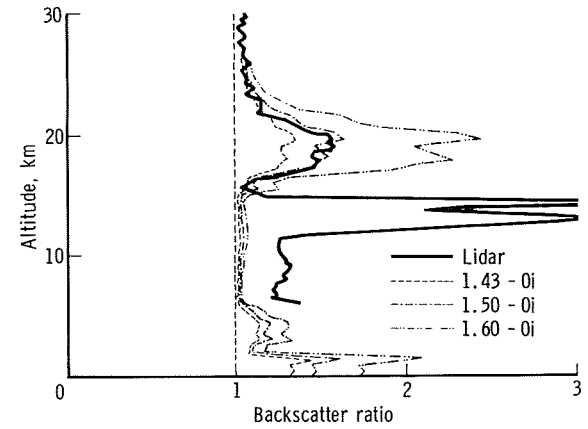

FIGURE 9-14.—Comparison of lidar results of July 22, 1975, and Mie computations of dustsonde results on July 22, 1975, for different optical properties of the aerosols.

size distribution fits to the dustsonde observations that were used for the previously mentioned SAM extinction dustsonde comparisons. The large enhancement at approximately 13 km in the July 22 lidar data is due to cirrus clouds.

Results of the three different techniques agree in the placement of the peak altitude of aerosol concentration, and they are consistent with a single size distribution and particle index. The

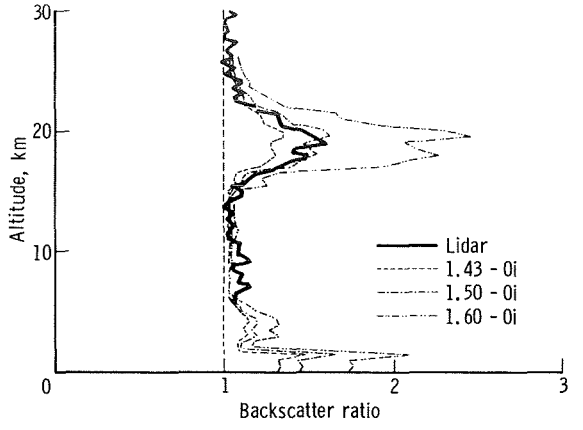

FIGURE 9-15.—Comparison of lidar results of July 23, 1975, and the Mie computations of dustsonde results on July 22, 1975, for different optical properties of the aerosols.

authors would like to point out that the log-normal distribution used to fit these observations is not necessarily unique. Other distributions might fit as well. For example, if the total number density of stratospheric aerosols is assumed to be 10 particles/cm^3, then results of the three different techniques are found to agree with a log-normal distribution for an aerosol index of refraction of 1.43, which is consistent with a sulfuric acid aerosol composed of 75 percent sulfuric acid and 25 percent water.

CONCLUSIONS

The SAM Experiment was performed by the ASTP crewmen as planned. The experiment demonstrated that solar occultation is a viable remote-sensing technique for measuring the verticle extinction of stratospheric aerosols. The solar photographs corroborated the refraction model needed for future solar occultation experiments. The inversion process that was used to reduce the SAM data was confirmed by the agreement with the ground-truth lidar and dustsonde measurements, and these data show that the solar occultation, lidar, and dustsonde data agree in altitude distribution and in yielding a consistent stratospheric aerosol size distribution model. In addition, the inversions from the SAM Experiment show a significant difference between the Northern and Southern Hemispheres with peak aerosol concentration at least 1.5 times greater in the Northern Hemisphere than in the Southern Hemisphere during the time of the ASTP flight.

REFERENCES

9-1. Rosen, James: Simultaneous Dust and Ozone Soundings Over North and Central America. J. Geophys. Res., vol. 73, no. 2, Jan. 15, 1968, pp. 479-486.

9-2. McCormick, M. P.; and Fuller, W. H., Jr.: Lidar Applications to Pollution Studies. Paper presented at Joint Conference on Sensing of Environmental Pollutants (Palo Alto, Calif.), Nov. 8-10, 1971. (AIAA Paper 71-1056.)

9-3. McCormick, M. P.; and Fuller, W. H., Jr.: Lidar Measurements of Two Intense Stratospheric Dust Layers. Appl. Opt., vol. 14, no. 1, Jan. 1975, pp. 4-5.

9-4. Cunnold, D.; Alyea, F.; Phillips, N.; and Prinn, R.: A Three-Dimensional Dynamical-Chemical Model of Atmospheric Ozone, J. Atmos. Sci., vol. 32, no. 1, Jan. 1975, pp. 170-194.

9-5. Pinnick, R. G.; Rosen, J. M.; and Hofmann, D. J.: Stratospheric Aerosol Measurements III: Optical Model Calculations. J. Atmos. Sci., vol. 33, no. 2, Feb. 1976, pp. 304-314.